



Aalborg Universitet

AALBORG UNIVERSITY  
DENMARK

## Parameters Uncertainty Immunization of Global Synchronous Pulse Width Modulated VSIs with Round P&O Algorithm

Xu, Tao; Gao, Feng; Tan, Pengfei; Meng, Xiangjian; Blaabjerg, Frede

*Published in:*  
I E E Transactions on Power Electronics

*DOI (link to publication from Publisher):*  
[10.1109/TPEL.2020.2982763](https://doi.org/10.1109/TPEL.2020.2982763)

*Publication date:*  
2020

*Document Version*  
Accepted author manuscript, peer reviewed version

[Link to publication from Aalborg University](#)

*Citation for published version (APA):*  
Xu, T., Gao, F., Tan, P., Meng, X., & Blaabjerg, F. (2020). Parameters Uncertainty Immunization of Global Synchronous Pulse Width Modulated VSIs with Round P&O Algorithm. *I E E Transactions on Power Electronics*, 35(11), 11281-11286. Article 9044772. <https://doi.org/10.1109/TPEL.2020.2982763>

### General rights

Copyright and moral rights for the publications made accessible in the public portal are retained by the authors and/or other copyright owners and it is a condition of accessing publications that users recognise and abide by the legal requirements associated with these rights.

- Users may download and print one copy of any publication from the public portal for the purpose of private study or research.
- You may not further distribute the material or use it for any profit-making activity or commercial gain
- You may freely distribute the URL identifying the publication in the public portal -

### Take down policy

If you believe that this document breaches copyright please contact us at [vbn@aub.aau.dk](mailto:vbn@aub.aau.dk) providing details, and we will remove access to the work immediately and investigate your claim.

# Parameters Uncertainty Immunization of Global Synchronous Pulse Width Modulated VSIs with Round P&O Algorithm

Tao Xu, *Member, IEEE*, Feng Gao, *Senior Member, IEEE*, Pengfei Tan, Xiangjian Meng, *Student Member, IEEE*, Frede Blaabjerg, *Fellow, IEEE*

**Abstract**—This paper proposes a closed-loop scheme for global synchronous pulse width modulated (GSPWM) voltage source inverters (VSIs) with round perturbation and observation (R-P&O) algorithm to immunize the parameters uncertainty, e.g. line impedance and filter impedance variation. In specific, the RMS value of measured total current harmonics at PCC will be periodically sent to each inverter as feedback signal using the low-cost narrowband communication system. Then, the inverters will assume the R-P&O scheme to correct the phase shift angles among PWM carriers for intentionally minimizing the total current harmonics. Doing so, the closed-loop scheme can achieve the expected performance even under the severe parameters' variation. The experimental results verified the performance of the proposed method.

**Keywords**—parameters uncertainty immunization; global synchronous pulse width modulation; parallel-connected inverters; closed-loop control

## I. INTRODUCTION

The voltage source inverters (VSIs) have been widely implemented in many applications, such as PV plants, wind plants and battery energy storage stations to integrate the distributed power sources to power grid [1]. The accumulated switching current harmonics at the point of common coupling (PCC) can be attenuated by assuming the interleaved pulse width modulation (PWM) sequences. Traditionally, the centralized PWM interleaving method can attenuate the current harmonics but is not adaptive to the distributed inverters [2–3]. Some decentralized method can realize the carrier interleaving without using central controller but can only be used in DC converters [4–5]. The recently proposed global synchronous pulse width modulation (GSPWM) method [6] provides a feasible operation scheme by coordinating the PWM sequences among paralleled VSIs. Besides, references [7–8] proposed a phase-locked-loop based carrier synchronization (PLL-CS) method for GSPWM, which

Manuscript received Feb. 11, 2020; revised Mar. 06, 2020; accepted Mar. 17, 2020. This work was supported in part by the China Postdoctoral Science Foundation under Grant 2019TQ0183 and Grant 2019M662358; in part by the National Natural Science Foundation of China under Grant 51722704; in part by the Shandong Provincial Natural Science Foundation, China, under Grant JQ201717; in part by the Foundation for Innovative Research Groups of National Natural Science Foundation of China under Grant 61821004 and in part by the Key Project of National Natural Science Foundation of China under Grant 61733010.

Corresponding author: Feng Gao

T. Xu, F. Gao P. Tan and X. Meng are with the Key Lab of Power System Intelligent Dispatch and Control of Ministry of Education, Jinan 250061, China (E-mail: txu@sdu.edu.cn).

F. Blaabjerg are with the Department of Energy Technology, Aalborg University, Denmark.

significantly improves the operational adaptivity because it makes the GSPWM not rely on the low-latency communication channels.

Another important issue of PWM interleaving is the calculation of carrier phase shift angles. For inverters with totally identical parameters, the phase shift angles can be easily obtained [9]. For the inverters with different parameters, e.g. different inductance, output power, switching frequencies, the GSPWM method can calculate their optimal phase shift angles to minimize the total current harmonics according to the pre-known parameters [6], which is referred to the open-loop scheme. But in practice, some inverters' parameters cannot be measured accurately during operation, e.g. the filter impedance and the feeder impedance. As a consequence, the reported phase shift angle calculation methods, which merely assume the open-loop control principle, cannot exactly guarantee the high frequency current harmonics attenuation as expected.

This paper therefore proposes a closed-loop scheme to guarantee the accurate harmonic attenuation by periodically capturing the RMS value of total current harmonics and adjusting the carriers' phase shift angles discontinuously using the round perturbation and observation (R-P&O) method for GSPWM-VSIs. Doing so, the closed-loop scheme can achieve the wide adaptability in implementations even without knowing the accurate inverters' parameters. Experimental results verified the performance of the proposed scheme.

## II. PERFORMANCE ANALYSIS OF TRADITIONAL OPEN-LOOP GSPWM SCHEME WITH INACCURATE PARAMETERS

In this section, the performance of traditional GSPWM operational principle will be briefly analyzed when the line parameters are not accurate in calculation.

In the following,  $N$  and  $m$  ( $m=1, \dots, N$ ) indicate the quantity and the number of inverters.  $\varphi_{m,PWM}$  indicates the phase shift angle between  $PWM_m$  and  $PWM_1$ , where  $PWM_m$  and  $PWM_1$  refer to the PWM sequences of inverter  $m$  and inverter 1, respectively. The range of  $\varphi_{m,PWM}$  is from  $0^\circ$  to  $360^\circ$ . Besides, the variables with subscript  $c$  indicate the calculated values according to the theoretical model with inaccurate parameters. And the variables with subscript  $a$  indicate the calculated values by employing the accurate parameters.

When using the open-loop scheme, the calculated optimal phase shift angle  $\varphi_{m,PWM,c}$  is obtained by minimizing RMS value of total current harmonics [6]:

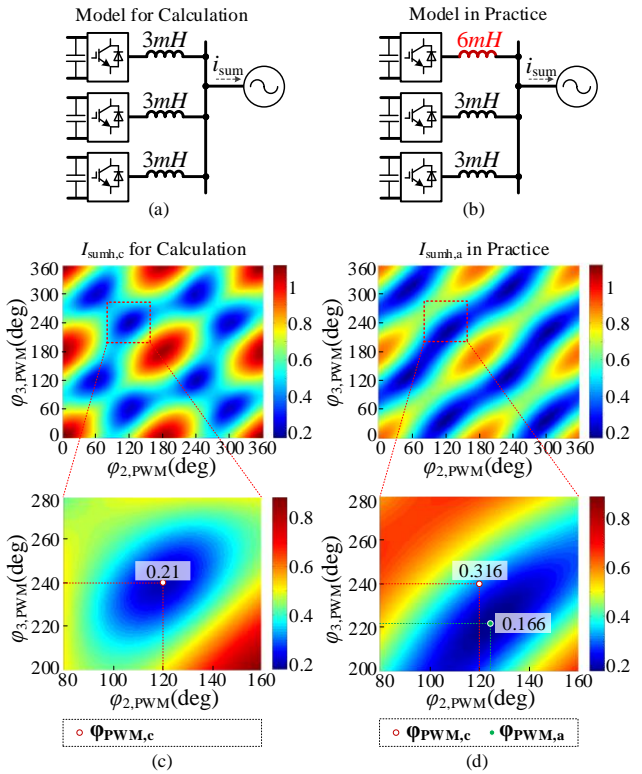


Fig. 1. Calculation models with (a) inaccurate and (b) accurate parameters, and (c)  $I_{sumh,c}$  and  $\varphi_{m,PWM,c}$  in theory and (d)  $I_{sumh,a}$  and  $\varphi_{m,PWM,a}$  in practice of three parallel-connected inverters.

$$\min I_{sumh,c} = \sqrt{\sum_{f=f_0+1}^{\infty} \left| \sum_{m=1}^N I_{m,hf,c} e^{j\varphi_{m,hf,c}(\varphi_{m,PWM,c})} \right|^2}$$

$$\text{s.t. } 0^\circ \leq \varphi_{m,PWM,c} \leq 360^\circ$$

$$I_{m,hf,c} = \frac{\dot{U}_{m,hf,c}}{Z_{m,out}}$$

where,  $I_{sumh,c}$  indicates the calculated RMS value of total current harmonics.  $I_{m,hf,c}$  indicates the calculated RMS value of harmonics flowing from inverter  $m$  with frequency  $f$ , which is derived according to harmonic voltage  $\dot{U}_{m,hf,c}$  and the pre-known output impedance  $Z_{m,out}$ .  $\dot{U}_{m,hf,c}$  can be derived using Double Fourier Method [10].

But in practice,  $Z_{m,out}$  contains the reactance of output filter and the estimated feeder impedance. The estimated feeder impedance is not always exactly equal to the real output impedance since the equivalent impedance under different high frequencies are totally different [11-12] and affected by the ambient temperature. So,  $\Phi_{PWM,c}$  which is the vector of all  $\varphi_{m,PWM,c}$  is also not equal to the wanted accurate optimal phase angles  $\Phi_{PWM,a}$  and the high frequency harmonics of total current at PCC will not be minimized as expected. To clearly illustrate this phenomenon, a simple example with three inverters is assumed, where the inverters' parameters except the output impedance are assumed to be identical. The calculation model with inaccurate parameters is shown in Fig. 1(a). Fig. 1(c) illustrates  $I_{sumh,c}$  under all the possible combinations of  $[\varphi_{1,PWM,c}, \varphi_{2,PWM,c}, \varphi_{3,PWM,c}]$ , where the color in figure indicates the value of  $I_{sumh,c}$ .  $\varphi_{1,PWM}$  is not shown here because it is set to  $0^\circ$  as the reference. The calculated  $\Phi_{PWM,c}$  in this example is  $[0^\circ, 120^\circ, 240^\circ]$ . But after measuring the real filter value of each inverter, the accurate model is shown in Fig. 1(b). The measured  $I_{sumh,a}$  under different phase

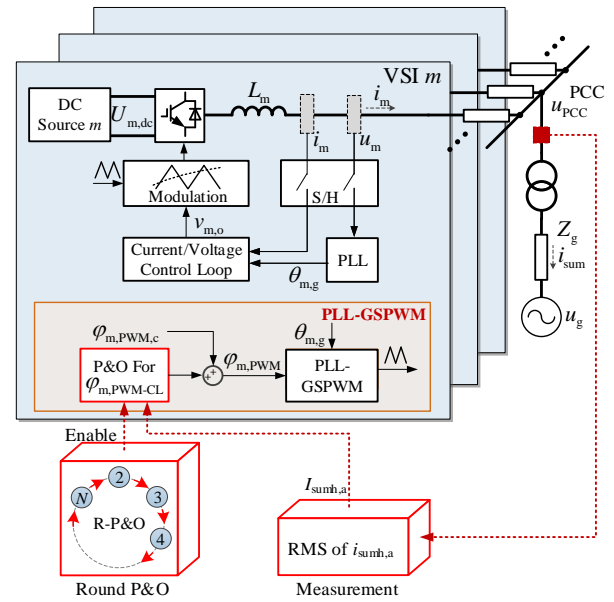


Fig. 2. Illustration of paralleled inverters with the proposed closed-loop scheme.

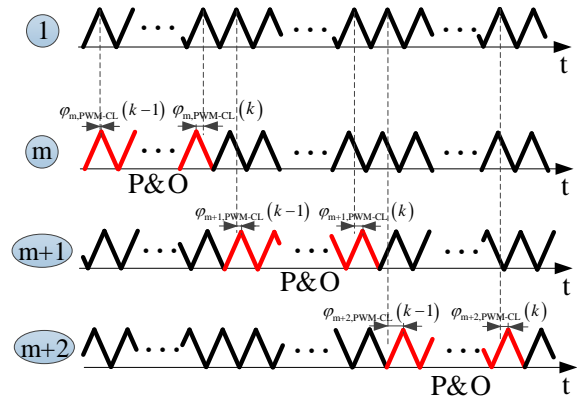


Fig. 3. Illustration of  $\varphi_{m,PWM-CL}$  using R-P&O.

angle combinations are shown in Fig. 1(d), where  $\Phi_{PWM,a}$  is  $[0^\circ, 125^\circ, 222^\circ]$ . It is obvious that  $\Phi_{PWM,c}$  deviates from  $\Phi_{PWM,a}$  because of the inaccurate parameters. If the inaccurate  $\Phi_{PWM,c}$  is used in practice,  $I_{sumh,a}$  will be 0.316 A as shown in Fig. 1(d) instead of the theoretically calculated 0.21 A in Fig. 1(c), though the real minimum value of  $I_{sumh,a}$  is 0.166 A. So, the existing open-loop scheme cannot track  $I_{sumh,a}$  properly when suffering the large parameter variation.

### III. PRINCIPLES AND REALIZATION OF CLOSED-LOOP SCHEME

To improve the control accuracy when using GSPWM, the closed-loop scheme will be fully elaborated below. In principle, a measurement unit is used to sample  $I_{sumh,a}$  and send to each inverter as shown in Fig. 2. Then, the coordination unit assumes the round perturbation and observation (R-P&O) algorithm to coordinate the switching sequences among inverters.

In specific, a current sensor is installed to measure the total current harmonics  $i_{sumh,a}$  at PCC. Then  $I_{sumh,a}$  can be simply derived and feedback to each inverter with the updating frequency  $f_{CL}$ . Since  $I_{sumh,a}$  is a specific value, it can be easily transmitted using the low-cost narrowband communication system. To be noted, the switching harmonics can be easily sampled because the sampling frequency could be set up to several hundred kHz. Upon inverters receive

$I_{\text{sumh},a}$ ,  $I_{\text{sumh},a}$  will be employed as the feedback value to generate the compensating phase shift angles to correct  $\varphi_{m,\text{PWM}}$  as expressed in (2).

$$\varphi_{m,\text{PWM}} = \varphi_{m,\text{PWM},c} + \varphi_{m,\text{PWM-CL}} \quad (2)$$

where,  $\varphi_{m,\text{PWM-CL}}$  indicates the compensating phase shift angles for inverter  $m$ .  $\varphi_{1,\text{PWM-CL}}$  is still set as  $0^\circ$ . Doing so,  $I_{\text{sumh},a}$  is given as:

$$I_{\text{sumh},a} = \sqrt{\sum_{f=f_0+1}^{\infty} \left| \sum_{m=1}^N I_{m,\text{hf},a} e^{j\varphi_{m,\text{hf},a}(\varphi_{m,\text{PWM},c} + \varphi_{m,\text{PWM-CL}})} \right|^2} \quad (3)$$

Compared with the model built in (1),  $\varphi_{m,\text{PWM-CL}}$  cannot be directly calculated by minimizing  $I_{\text{sumh},a}$  because the parameters in (3), such as  $I_{m,\text{hf},a}$ , cannot be obtained accurately. So the perturbation and observation method can be assumed to find the optimal  $\varphi_{m,\text{PWM-CL}}$ . According to the model of (3),  $I_{\text{sumh},a}$  is determined by  $\varphi_{m,\text{PWM-CL}}$  of all inverters. That means, if all the inverters operate P&O together, it will be hard for each inverter to determine the changing direction of  $\varphi_{m,\text{PWM-CL}}$ .

In order to find  $\varphi_{m,\text{PWM-CL}}$ , the R-P&O scheme is proposed, which only perturbs one  $\varphi_{m,\text{PWM-CL}}$  each time as shown in Fig. 3. When using the R-P&O,  $I_{\text{sumh},a}$  is given as:

$$I_{\text{sumh},a} \left( \begin{matrix} \varphi_{m,\text{PWM-CL}} \\ \pm \Delta \varphi_{m,\text{PWM-CL}} \end{matrix} \right) = \sqrt{\sum_{f=f_0+1}^{\infty} \left| \sum_{i=1}^N I_{i,\text{hf},a} e^{j\varphi_{i,\text{hf},a}(\varphi_{m,\text{PWM},c} + \varphi_{m,\text{PWM-CL}}(k))} \right|^2} \quad (4)$$

where,  $I_{\text{sumh},a}$  is dependent on  $\varphi_{m,\text{PWM-CL}}(k)$  because other  $\varphi_{i,\text{PWM-CL}}(i \neq m)$  are unchanged. The perturbation will begin with the initial  $\varphi_{m,\text{PWM-CL}}(0)$  being  $0^\circ$ . In order to determine the updating direction of  $\varphi_{m,\text{PWM-CL}}(k)$ , the  $\varphi_{m,\text{PWM-CL}}(k)$  is perturbed to the following three values one after another:

$$\begin{aligned} \varphi_{m,\text{PWM-CL}}(k) &= \varphi_{m,\text{PWM-CL}}(k-1); \\ \varphi_{m,\text{PWM-CL}}(k) &= \varphi_{m,\text{PWM-CL}}(k-1) + \Delta \varphi_{m,\text{PWM-CL}}; \\ \varphi_{m,\text{PWM-CL}}(k) &= \varphi_{m,\text{PWM-CL}}(k-1) - \Delta \varphi_{m,\text{PWM-CL}}; \end{aligned} \quad (5)$$

where,  $\Delta \varphi_{m,\text{PWM-CL}}$  indicates the perturbation step. During the perturbation, the measurement unit measures  $I_{\text{sumh},a}$  and sends  $I_{\text{sumh},a}$  to inverter  $m$ . Then inverter  $m$  can update  $\varphi_{m,\text{PWM-CL}}(k)$  to the value who leads to the minimum  $I_{\text{sumh},a}$ . The  $\varphi_{m,\text{PWM-CL}}(k)$  is updated one time during each P&O operation, then the P&O operation will be triggered in inverter  $m+1$ . After finishing P&O operation for inverter  $N$ , the P&O will be employed again from inverter 2 to inverter  $N$  and repeat the above procedures. The sequence diagram of the closed-loop scheme is shown in Fig. 4, where the measurement operates all the time while P&O operates from one inverter to next inverter.

The example with 3 inverters shown in Fig. 1(b) is still employed here to briefly illustrate the closed-loop scheme. The calculated  $\Phi_{\text{PWM},c}$  is  $[0^\circ, 120^\circ, 240^\circ]$  and the initial  $\varphi_{m,\text{PWM-CL}}(0)$  is  $0^\circ$ .  $\Delta \varphi_{m,\text{PWM-CL}}$  is assumed as  $5^\circ$ . Firstly, only  $\varphi_{2,\text{PWM-CL}}$  is perturbed while  $\varphi_{3,\text{PWM-CL}}$  is fixed at  $0^\circ$  as shown in the left figure of Fig. 5(a). After comparing  $I_{\text{sumh},a}$  for  $\varphi_{2,\text{PWM-CL}} = -5^\circ, 0^\circ, +5^\circ$ , inverter 2 updates the  $\varphi_{2,\text{PWM-CL}}$  to  $+5^\circ$  who produces the minimum  $I_{\text{sumh},a}$ . The right figure of Fig. 5(a) shows the updating trajectory of  $\varphi_{2,\text{PWM-CL}}$ . Then, only  $\varphi_{3,\text{PWM-CL}}$  is perturbed while the  $\varphi_{2,\text{PWM-CL}}$  is fixed at  $5^\circ$  as shown in the left figure of Fig. 5(b). Being similar to the P&O procedures for  $\varphi_{2,\text{PWM-CL}}$ , the  $\varphi_{3,\text{PWM-CL}}$  is updated as

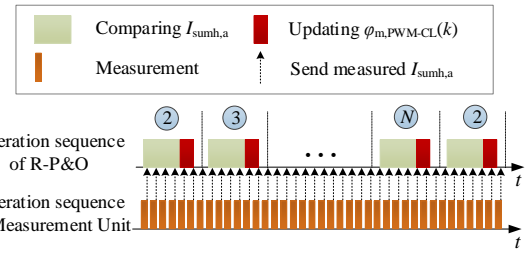


Fig. 4. Operation sequences of R-P&O and measurement unit when the proposed closed-loop scheme is employed.

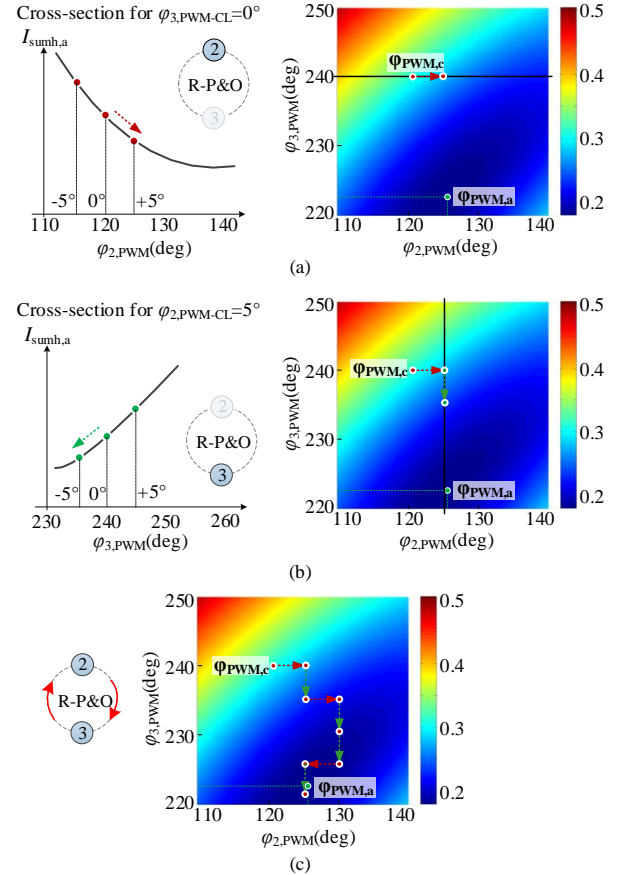


Fig. 5. Illustration of R-P&O for 3 inverters. (a) When only perturbate  $\varphi_{2,\text{PWM-CL}}$  while keep  $\varphi_{3,\text{PWM-CL}}$  fixed. (b) When only perturbate  $\varphi_{3,\text{PWM-CL}}$  while keep  $\varphi_{2,\text{PWM-CL}}$  fixed. (c) The whole trajectory of  $\varphi_{m,\text{PWM}}$ .

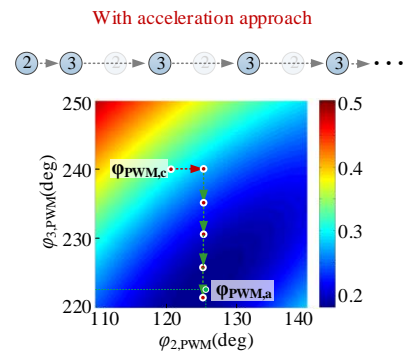


Fig. 6. The trajectory of  $\varphi_{m,\text{PWM}}$  for 3 inverters with acceleration approach.

$-5^\circ$ . The right figure of Fig. 5(b) shows the updating trajectory of  $\varphi_{3,\text{PWM-CL}}$ . Then repeating P&O for inverters 2 and 3,  $I_{\text{sumh},a}$  will approach the real minimum value as shown in Fig. 5(c).

To avoid the locally-optimal solutions,  $\varphi_{m,\text{PWM},c}$  should be pre-calculated. Fortunately,  $\varphi_{m,\text{PWM},c}$  is close to the  $\varphi_{m,\text{PWM},a}$ ,

**TABLE I EXPERIMENTAL PARAMETERS**

$m$	$U_{m,dc}/V$	$L_m/mH$	$f_{m,c}$
1	170 V	6 mH	10 kHz
2	165 V	3 mH	10 kHz
3	168 V	3 mH	10 kHz

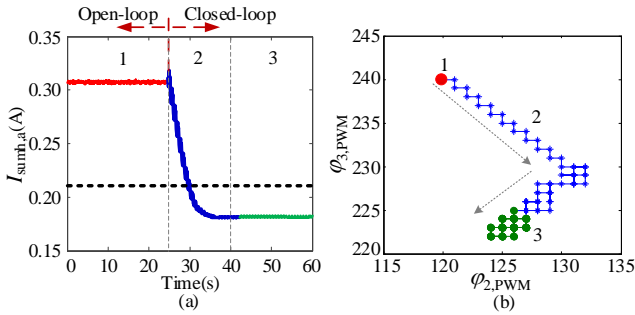


Fig. 7 (a) Trajectory of  $I_{sum,h,a}$ . (b) Trajectory of  $\phi_{m,PWM}$ .

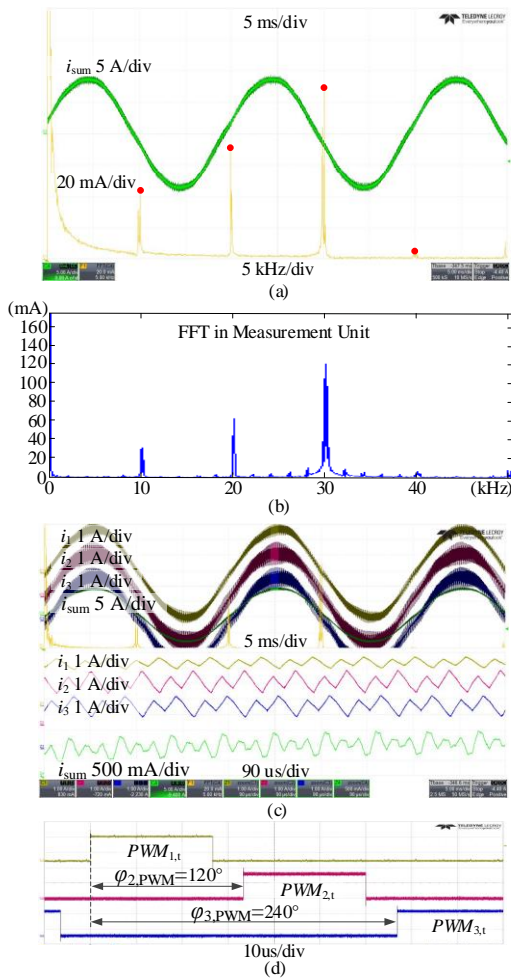


Fig. 8. Experimental waveforms of OL-GSPWM with (a)  $I_{sum,h,a}$  and FFT spectrum, (b) FFT results in measurement unit, (c)  $i_1, i_2, i_3, i_{sum,h,a}$  and the zoomed view and (d) measured  $\phi_{m,PWM}$ .

which can help the round P&O algorithm to track the optimal values. Then, the round P&O with variable steps can be used. In principle, the variable steps are set as large value initially and then decrease [13-15].

On the other hand, in order to reduce the tracking time when the number of inverter is large, the sequences of P&O operation can be rearranged according to the gradient of last

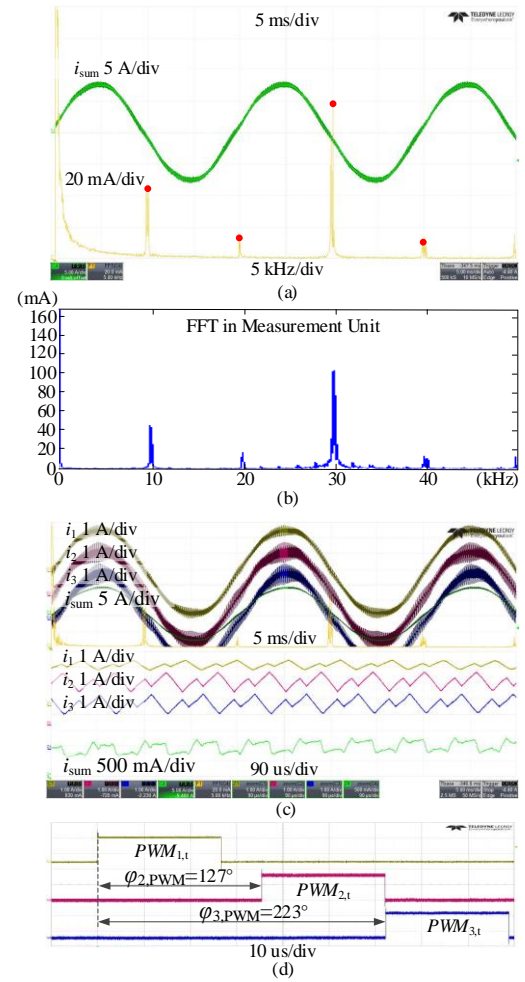


Fig. 9. Experimental waveforms of CL-GSPWM with (a)  $I_{sum,h,a}$  and FFT spectrum, (b) FFT results in measurement unit, (c)  $i_1, i_2, i_3, i_{sum,h,a}$  and the zoomed view and (d) measured  $\phi_{m,PWM}$ .

P&O operation. The gradients of  $I_{sum,h,a}$  when using P&O operation in different inverters are calculated and compared. Then the inverter whose last P&O operation leads to the maximum gradient will be enabled. Fig. 6 shows the trajectory of  $\phi_{m,PWM}$  with this kind of acceleration approach. The gradients of last P&O operation in inverter 2 and inverter 3 are compared. The P&O operation in inverter 3 leads to larger gradient, so the P&O algorithm will run again in inverter 3. Comparing Fig. 6 and Fig. 5(c), the superiority of acceleration procedure is obvious.

#### IV. EXPERIMENTAL VERIFICATION

The constructed experimental prototype has 3 three-phase two-level voltage source inverters (VSI) with their own independent DC sources, output filters and digital controllers. The used DSP is TMS320F28335. The inverters parameters are listed in Table 1. All inverters are connected to an emulated grid using a programmable AC source, whose RMS value of output voltage is 110 V and the rated output frequency is 50 Hz. The oscilloscope with 4 channels was used to record the waveforms. A measurement unit containing DSP and sensor board was used to measure and calculate  $I_{sum,h}$ . Firstly, the total current  $i_{sum}$  is measured and converted into low voltage signal by Hall sensor (LA100-P) and amplifier within the range of 0~3 V. Then the analog signal is

converted into digital signal by the Analog-to-Digital Converter (ADC) module of DSP (TMS320F28335). The sampling rate of ADC module is 102.4 kHz. A radix-2 FFT algorithm is running in this DSP, which converts the current samples to frequency domain after sampling 20 ms. Finally,  $I_{\text{sumh},a}$  can be easily derived according to the FFT results.  $I_{\text{sumh},a}$  will be sent to each inverter through the RS-485 communication channels in this experiment. The updating frequency of the measurement unit is set as 10 Hz.

In this experiment, the open-loop scheme is used from 0 s to 25 s and the proposed closed-loop scheme is assumed from 25 s to 60 s. Fig. 7 shows the trajectories of  $I_{\text{sumh},a}$  and  $\phi_{m,\text{PWM}}$ . The trajectories are divided into 3 stages. In stage 1, the calculated  $I_{\text{sumh},c}$  is 0.21 A and the calculated  $\phi_{\text{PWM},c}$  is  $[0^\circ, 120^\circ, 240^\circ]$  in theory. But when employing  $\phi_{\text{PWM},c}$  in open-loop GSPWM, the measured  $I_{\text{sumh},a}$  is actually 0.31 A. That means the open-loop scheme underestimates the current harmonics and cannot control  $I_{\text{sumh},a}$  accurately. After using the proposed closed-loop scheme,  $\phi_{\text{PWM}}$  will change to  $[0^\circ, 127^\circ, 223^\circ]$  because  $\phi_{m,\text{PWM-CL}}$  is used to compensate  $\phi_{\text{PWM}}$  as shown in stage 2. After 10 s, the measured  $I_{\text{sumh},a}$  becomes 0.18 A, which approaches the minimum value as shown in stage 3.

Fig. 8 shows the experimental waveforms of the open-loop scheme in stage 1, while Fig. 9 shows the experimental waveforms of the closed-loop scheme in stage 3. Comparing the experimental results of open-loop scheme and closed-loop scheme, it is noted that the closed-loop scheme can approach the real minimum value. Besides, the FFT spectrum in Fig. 8 and 9 verified that the FFT results in measurement unit are equal to those calculated by the oscilloscope whose sampling frequency can be up to 50 MHz. So, the measurement unit is able to measure  $I_{\text{sumh},a}$  in practice.

## V. CONCLUSION

This paper proposes a closed-loop global synchronous pulse width modulation scheme with round perturbation and observation algorithm for paralleled voltage source inverters to immunize the parameters uncertainty. Experimental results verified the performance of the proposed method.

## REFERENCES

- [1] F. Blaabjerg, Z. Chen and S. B. Kjaer, "Power electronics as efficient interface in dispersed power generation systems," *IEEE Trans. Power Electron.*, vol. 19, no. 5, pp. 1184-1194, Sep. 2004.
- [2] M. A. Abusara, S. M. Sharkh, "Design and control of a grid-connected interleaved inverter," *IEEE Trans. Power Electron.*, vol.28, no. 2, pp. 748 - 764, Feb. 2013.
- [3] D. Zhang, F. Wang, R. Burgos, R. Lai, and D. Boroyevich, "Impact of interleaving on AC passive components of paralleled three-phase voltage-source converters," *IEEE Trans. Ind. Appl.*, vol. 46, no. 3, pp. 1042-1054, May/June. 2010.
- [4] M. Sinha, J. Poon, B. B. Johnson, M. Rodriguez, Sairaj V. Dhople, "Decentralized interleaving of parallel-connected buck converters," *IEEE Trans. Power Electron.*, vol. 34, no. 5, pp. 4993-5006, May. 2019.
- [5] D. Perreault and J. Kassakian, "Distributed interleaving of paralleled power converters," *IEEE Trans. Circuits Syst. I, Fundam. Theory Appl.*, vol. 44, no. 8, pp. 728-734, Aug. 1997.
- [6] T. Xu and F. Gao, "Global synchronous pulse width modulation of distributed inverters," *IEEE Trans. Power Electron.*, vol. 31, no. 9, pp. 6237-6253, Sep. 2016.
- [7] T. Xu, F. Gao, X. Wang and F. Blaabjerg, "A carrier synchronization method for global synchronous pulse width modulation application using phase-locked-loop," *IEEE Trans. Power Electron.*, vol. 34, no. 11, pp. 10720-10732, Nov. 2019.

- [8] J. He, Z. Dong, Y. Li, C. Wang, "Parallel-converter system grid current switching ripples reduction using a simple decentralized interleaving PWM approach," *IEEE Trans. Power Electron.*, 2019, early access.
- [9] B. Cougo, T. Meynard, and G. Gateau, "Parallel three-phase inverters: Optimal PWM method for flux reduction in intercell transformers," *IEEE Trans. Power Electron.*, vol. 26, no. 8, pp. 2184-2191, Aug. 2011.
- [10] D. G. Holmes and T. A. Lipo, "Pulse width modulation for power converters: Principles and practice", Wiley, New York, NY, USA, p 241-249.
- [11] S. Morched and P. Kundur, "Identification and modelling of load characteristics at high frequencies," *IEEE Trans. Power Syst.*, vol. 2, no. 1, pp. 153-159, Feb. 1987.
- [12] A. Girgis and R. B. McManis, "Frequency domain techniques for modeling distribution or transmission networks using capacitor switching induced transients," *IEEE Trans. Power Del.*, vol. 4, no. 3, pp. 1882-1890, July 1989.
- [13] J. Ahmed and Z. Salam, "An enhanced adaptive P&O MPPT for fast and efficient tracking under varying environmental conditions," *IEEE Trans. Sustain. Energy*, vol. 9, no. 3, pp. 1487-1496, July 2018.
- [14] J. Prasanth Ram and N. Rajasekar, "A novel flower pollination based global maximum power point method for solar maximum power point tracking," *IEEE Trans. Power Electron.*, vol. 32, no. 11, pp. 8486-8499, Nov. 2017.
- [15] W. Zhang, G. Zhou, H. Ni and Y. Sun, "A modified hybrid maximum power point tracking method for photovoltaic arrays under partially shading condition," *IEEE Access*, vol. 7, pp. 160091-160100, 2019.